

# 1 Enhancer RNA-based modeling of adverse events and objective responses of 2 immunotherapy

3

4 Mengbiao Guo<sup>1,\*</sup>, Zhiya Lu<sup>1,\*</sup>, Yuanyan Xiong<sup>1,#</sup>

5

6 <sup>1</sup>Key Laboratory of Gene Engineering of the Ministry of Education, Institute of Healthy Aging  
7 Research, School of Life Sciences, Sun Yat-sen University, Guangzhou 510006, China.

8 \* These authors contributed equally to this work.

9 # Corresponding author: [xyyan@mail.sysu.edu.cn](mailto:xyyan@mail.sysu.edu.cn), Tel: +86-20-39943531, Fax: +86-20-  
10 39943778

11

## 12 Abstract

13

14 Immune checkpoint inhibitors (ICI) targeting PD-1/PD-L1 or CTLA-4 are emerging and  
15 effective immunotherapy strategies. However, ICI treated patients present heterogeneous  
16 responses and adverse events, thus demanding effective ways to assess benefit over risk before  
17 treatment. Here, by integrating pan-cancer clinical and molecular data, we tried to predict  
18 immune-related adverse events (irAEs, risk) and objective response rates (ORRs, benefit)  
19 based on enhancer RNAs (eRNAs) expression among patients receiving anti-PD-1/PD-L1  
20 therapy. We built two effective regression models, explaining 71% variance ( $R=0.84$ ) of irAEs  
21 with three eRNAs and 79% ( $R=0.89$ ) of ORRs with five eRNAs. Interestingly, target genes of  
22 irAE-related enhancers, including upstream regulators of MYC, were involved in metabolism,  
23 inflammation, and immune activation, while ORR-related enhancers target *PAK2* and *DLG1*  
24 which directly participate in T cell activation. Our study provides references for the

25 identification of immunotherapy-related biomarkers and potential therapeutic targets during  
26 immunotherapy.

27

## 28 Introduction

29

30 Immune checkpoints (ICs) generally refer to key inhibitory factors of the immune system,  
31 including programmed cell death 1 (PD-1 or CD279) and its ligand programmed cell death 1  
32 ligand 1 (PD-L1 or CD274) that control the T cell response and fate during tumor immunity  
33 [1]. In tumor samples, PD-1 and PD-L1 mainly expressed in T cells and tumor cells,  
34 respectively, and tumors exploit their interaction to escape the immune system by  
35 counteracting the stimulatory signals from the interaction between T cell receptor (TCR) and  
36 major histocompatibility complex (MHC) and other costimulatory signals [2-4].

37

38 PD-1/PD-L1 has been translated to the clinical practice, and ICI treatment targeting PD-1/PD-  
39 L1 proved to offer significant clinical benefits in many cancers, with an ORR from 20% to 50%  
40 in multiple clinical trials and for various types of cancer [5]. However, only a small subset of  
41 patients showed long-lasting remission, despite remarkable benefits of ICI therapies. Patients  
42 of some cancers were completely refractory to checkpoint blockade, occasionally leading to  
43 considerable side effects. To predict treatment benefit, PD-L1 expression was proposed as the  
44 first biomarker of anti-PD-1/PD-L1 therapy effectiveness [6], followed by tumor mutational  
45 burden (TMB) [7]. Later, microsatellite instability (MSI) [8], CD8+ T-cell abundance [9, 10],  
46 cytolytic activity [11], and intestinal microbial composition[12] were proposed to prioritize  
47 patients with potentially more treatment gains.

48

49 On the other hand, irAEs result from excessive immunity against normal organs. Most studies  
50 show that the incidence of irAEs caused by anti-PD-1/PD-L1 treatment is about 60% [13, 14].  
51 Although nearly all organs can be affected, irAEs mostly involved the gastrointestinal tract,  
52 endocrine glands, skin, and liver [15]. In some cases, irAE can be lethal. For example,  
53 pneumonitis is the most common fatal irAE with a 10% death rate, accounting for 35% of anti-  
54 PD-1/PD-L1-related fatalities [16]. The mortality of myocarditis, the most lethal irAE, could  
55 even reach about 50% [17]. Therefore, it is important and urgent to select patients with  
56 potentially significant benefit over risk of ICI treatments based on individual molecular data.  
57 Although people have discovered several predictors of irAEs using expression of protein-  
58 coding genes [18], studying irAE-related non-coding elements would probably provide a better  
59 mechanistic understanding of why PD-1/PD-L1 pathway modulation leads to significant  
60 clinical benefit in some patients but temporary, partial, or no clinical benefit in other patients.  
61  
62 Recent studies found that eRNAs (non-coding RNAs) were usually transcribed from active  
63 enhancers and eRNA levels portended enhancer activities across tissues [19]. Numerous  
64 cancer-associated eRNAs have been identified and eRNAs were proposed as potential  
65 therapeutic targets [20]. Here, we comprehensively investigate the adverse events and the  
66 response rates in patients receiving anti-PD-1/PD-L1 therapies across cancer types. By  
67 integrating clinical data and molecular data, we identify predictors based on three eRNAs for  
68 predicting irAE and five eRNAs for ORR. Further exploring enhancer-target interaction  
69 identified functional genes that may help explain the overall risk or benefit of anti-PD-1/PD-  
70 L1 therapy, including MLXIPL, RAF1, MPL, PAK2, DLG1. In summary, our study reveals  
71 potential mechanisms underlying ICI therapy based on enhancer activity.

## 72 Results

73

### 74 **Three eRNAs effectively predict irAE of immunotherapy**

75

76 To identify factors to predict irAEs, we first examined correlations between 7 045 eRNAs and  
77 irAE RORs across 25 cancer types and found 178 eRNAs positively correlated with irAEs with  
78 nominal significance ( $P < 0.05$ ). Among these eRNAs, ENSR00000041252 showed the highest  
79 correlation (correlation  $R = 0.68$ ,  $P = 1.6e-4$ ; **Fig. S1A**), stronger than immune factors, including  
80 naive B cells, CD8+ T cells, macrophages M1, and T cell receptor diversity [18].

81

82 Then, we selected the top ten eRNAs (**Table S1**) to build prediction models. Multicollinearity  
83 analysis resulted in six roughly independent eRNAs, ENSR00000041252, ENSR00000326714,  
84 ENSR00000148786, X14.65054944.65060944, ENSR00000118775, and ENSR00000242410  
85 (**Fig. 1A** and **Fig. 1B**). Next, we obtained 15 significant bivariate regression models using the  
86 irAE-correlated enhancers. Correlation between the observed and predicted irAE ROR values  
87 showed that the combination ENSR00000148786 + ENSR00000005553 achieved the best  
88 predictive performance ( $R = 0.79$ ,  $P = 3.1e-6$ ; **Fig. S1B**). Further increasing model factors  
89 resulted in the optimal tri-variate model, ENSR00000041252 + ENSR00000148786 +  
90 ENSR00000005553, with the strongest correlation ( $R = 0.84$ ,  $P = 2.1e-6$ ; **Fig. 1C**). Of note, no  
91 improvement was observed after adding the two protein-coding genes (LCP1 and ADPGK)  
92 from a model reported previously [18], suggesting the independence of our model. Although  
93 showing slightly lower performance than the previous protein-coding gene model  
94 (LCP1+ADPGK), our enhancer-based model, explaining 71% (R-squared,  $R = 0.84$ ) of irAE  
95 variance, demonstrated that eRNAs alone can effectively predict irAEs.

96

### 97 **Five eRNAs effectively predict immunotherapy benefit**

98

99 Similarly, to identify factors to predict ORRs, we identified 28 out of 7 045 eRNAs positively  
100 correlated with ORR ( $P < 0.05$ ; the best one ENSR00000187665 shown in **Fig. S1C**). Based on  
101 the top ten eRNAs (**Table S2**), after multicollinearity analysis (**Fig. 1D** and **Fig. 1E**), two  
102 bivariate models achieved better predictive performance than single-eRNA models (one shown  
103 in **Fig. S1D**;  $R = 0.82$ ,  $P = 2.0e-5$ ). Further adding model factors resulted in four equally-efficient  
104 optimal trivariate models (involving five key eRNAs, **Table S3**) for ORR prediction were able  
105 to effectively predict the efficacy of anti-PD-1/PD-L1 treatments. One example,  
106 ENSR00000164478 + ENSR00000035913 + ENSR00000167231, was shown in **Fig. 1F**  
107 ( $R = 0.89$ ,  $P = 3.3e-7$ ).

108

### 109 **Enhancer-target networks of irAE and ORR-associated enhancers**

110

111 Enhancers were assumed to affect irAEs or ORRs by activating target genes through long-  
112 range interactions. We downloaded enhancer-target interaction data[21] and obtained putative  
113 targets of our enhancers. Two eRNAs (ENSR00000262415 and ENSR00000167231) were  
114 excluded from downstream analysis due to lack of any annotated target gene. eRNA-target  
115 networks showed that these enhancers independently regulated a specific groups of targets (**Fig.**  
116 **2A** and **Fig. 2B**, note that ENSR00000164478 and ENSR00000164479 located to the same  
117 genomic region), indicating that each irAE-related enhancer was involved in different  
118 regulatory modules. Similarly, protein-protein interaction (PPI) analysis revealed that an  
119 independent network was controlled by each enhancer (**Fig. 1C** and **Fig. 1D**). In these PPI  
120 networks, genes located in the center (such as BCL7B, TBL2, and NAP1L4) might be vital  
121 regulators of irAEs or ORRs.

122

### 123 **Enhancer targets reveal metabolic and inflammatory genes involved in irAEs**

124

125 Next, we downloaded gene sets from COSMIC[22] and oncoKB[23] and examined our eRNA  
126 targets in known oncogenic signaling pathways using cBioPortal[24, 25]. We found that some  
127 eRNA targets were known cancer genes relevant to tumor immunity, including *MLXIPL*, *MPL*,  
128 *RAF1*, and *XPC*. *RAF1* was annotated as an oncogene and participated in the RTK-RAS  
129 signaling pathway (**Fig. S2A**) and *MLXIPL* was involved in MYC signaling pathway (**Fig.**  
130 **S2B**). A previous work[26] shows *RAF1* can activate MAPK1 and NF- $\kappa$ B pathways to regulate  
131 genes involved in inflammation. Therefore, *RAF1* may enhance immunoreaction and  
132 subsequently cause irAEs via Natural Killer cell-mediated cytotoxicity, T cell receptor  
133 signaling pathway, and B cell receptor signaling pathway.

134

135 Interestingly, we found that ENSR00000326714 targets were enriched in a large number of  
136 metabolic and biosynthesis processes (**Fig. 2E**). This was reminiscent of some types of adverse  
137 events, such as diabetes[16], due to metabolic disturbances or metabolic disorders. Specifically,  
138 the core network of ENSR00000326714 targets consists of seven metabolic and inflammatory  
139 genes, namely, *BAZ1B*, *BCL7B*, *TBL2*, *MLXIPL*, *NSUN*, *STX1A*, and *VPS37D*. Among  
140 them, *BAZ1B*, *BCL7B*, *TBL2* and *MLXIPL* are pleiotropic genes for lipids and inflammatory  
141 markers in the liver[27]. Of note, *MLXIPL* encodes the carbohydrate-responsive element-  
142 binding protein (ChREBP), which mediates glucose homeostasis and liver lipid metabolism.  
143 ChREBP was also associated with up-regulation of several cytokines (TNF- $\alpha$ , IL-1 $\beta$ , and IL-  
144 6) in patients with type 2 diabetes mellitus, promoting the inflammatory responses and  
145 apoptosis of mesangial cells[28]. *STX1A* encodes a member of the syntaxin superfamily,  
146 syntaxin 1A. It contributes to neural function in the central nervous system by regulating  
147 transmitter release[29]. As a kind of target-SNAP receptor (t-SNAREs), it is involved in insulin  
148 exocytosis[30]. Severely reduced islet syntaxin 1A level was reported to contribute to insulin

149 secretory deficiency[31]. Given that diabetes and hepatitis account for ~30% of immune-  
150 related adverse events[16], we speculate that ENSR00000326714 augmented the expression of  
151 the these genes, subsequently triggering inflammation and other toxic effects on these patients.

152

### 153 **ORR enhancers reveal immune activation genes for immunotherapy benefit**

154

155 We also analyzed target genes of ORR-predictable eRNAs (**Fig. 2B**), which included three  
156 types of genes. PAK2, LMLN, DLG1, ASCL2, SENP5, IQCG, and BRSK2 are related to cell  
157 cycle, cell division, and differentiation. PIGZ, PIGX, PCYT1A, CARS, and BDH1 are  
158 metabolic genes; TRPM5, KCNQ1, and FYTTD1 are responsible for cellular transport and  
159 signal transduction. In particular, target genes of ORR-related ENSR00000164478 were  
160 enriched in glycosylphosphatidylinositol (GPI)-anchor biosynthesis ( $FDR=4.73\times 10^{-3}$ ) (**Fig. 2F**)  
161 and T-cell receptor signaling ( $FDR=3.78\times 10^{-2}$ ), among other enriched pathways (**Fig. 2G**).

162

163 Furthermore, PAK2 and DLG1 directly took part in the T cell activation pathway, which  
164 explains their connection with ORR. P21 (RAC1) activated kinase 2 (PAK2) has been reported  
165 as a key signaling molecule in the differentiation of T cells. PAK2 is essential in T cell  
166 development and differentiation[32], indicating its potential function in T cell-initiated  
167 autoimmunity. DLG1 encodes a multi-domain scaffolding protein from the membrane-  
168 associated guanylate kinase family, which has been shown to regulate the antigen receptor  
169 signaling and cell polarity in lymphocytes, involved in activation and proliferation of T cells[33,  
170 34]. Our results provide more support for the T cells as the regulators in immune responses  
171 during immune checkpoint blockade therapy.

172 Lastly, PIGZ encodes a protein that is previously identified as an immune-associated prognosis  
173 signature[35]. However, knowledge of the relationship between PIGZ and the immune system

174 is still poorly established. The association between PIGZ expression and immune benefits  
175 during anti-PD1/PDL1 immunotherapy needs further elucidation.

176

## 177 Discussions

178

179 In this work, we presented a preliminary evaluation of the different enhancer-target interactions  
180 associated with anti-PD-1/PD-L1 immunotherapy across tumor types, and successfully  
181 identify potential enhancer-based biomarkers of risk and beneficial response. We suggest that,  
182 during immunotherapy, enhanced expression of inflammatory factors including MLXIPL,  
183 STX1A, and RAF1 may lead to a higher risk of irAEs, while strengthening immune activation  
184 factors including PAK2 and DLG1 may improve anti-tumor immunity. Besides, we discovered  
185 many other cancer-related, metabolic, signaling or regulatory genes possess predictive  
186 potential, which warrants further investigation.

187

188 Several limitations remain for future work and our results need to be carefully interpreted. First,  
189 the majority of data are collected from previous individual studies[21], introducing inherent  
190 limitations of their work. Second, there are inevitable flaws of modeling as well, due to the low  
191 expression level of eRNA and small sample size. The overall quality of predictive models of  
192 ORR is inferior to those of irAEs, probably due to a smaller sample size as well as larger  
193 sparsity of ORR data. Finally, since results in this project are mainly based on computational  
194 predictions and the support of existing literature, our findings need further experimental  
195 validation. A larger dataset is required to comprehensively model side effects or immune  
196 response as well.

197



## 198 **Methods**

199

### 200 **Data collection**

201 To quantify the risk of immune-related adverse events (irAEs), reporting odds ratio (ROR) was  
202 calculated as previously described [36]. The anti-PD1/PD-L1 irAE ROR and ORR values  
203 across different cancer types were collected from previous studies [10, 18]. RNA-seq  
204 expression data (RSEM normalized counts, log<sub>2</sub>-transformed) across 25 TCGA cancers were  
205 downloaded from the UCSC Xena platform (<http://xena.ucsc.edu/>). Expression levels of  
206 selected genes were extracted for downstream analysis, and the average value was calculated  
207 for each TCGA cohort. We downloaded eRNA expression levels and enhancer-target  
208 associations for 7 045 enhancer RNAs in ~7,300 samples from the eRic database [21]  
209 (<https://hanlab.uth.edu/eRic/>). Mean eRNA expression (log<sub>2</sub>-transformed RPM values) were  
210 used. Similar to gene expression, we averaged the expression level of each eRNA for each  
211 cancer.

212

### 213 **Prediction model construction**

214 First, the top ten eRNAs were selected based on correlation between eRNA and irAE or ORR.  
215 Before constructing bivariate models, the variance inflation factor[37] (VIF) of these ten  
216 eRNAs was calculated to evaluate the multicollinearity. Generally, we set the threshold of VIF  
217 value to 4 (a VIF value greater than 10 will be considered serious multicollinearity). The  
218 optimal prediction model was obtained by step-wise addition of model factors (eRNA) and  
219 evaluate the correlation between predicted and observed patient risk or benefits.

220

### 221 **Bioinformatics tools**

222 We used the protein-protein interaction (PPI) database STRING[38] (v11, <https://string-db.org>)  
223 to investigate selected eRNA target genes. Basic GO and KEGG term enrichment and  
224 visualization were conducted with the R package clusterProfiler[39] (v3.14.3). Extensive  
225 functional annotation of eRNA target genes were performed with DAVID [40] (v6.8)  
226 (<https://david.ncifcrf.gov/>). To verify cancer-related function for genes of interest, a credible  
227 set of 723 cancer genes was downloaded from the Cancer Gene Census (CGC) project of the  
228 COSMIC[22] repository (<https://cancer.sanger.ac.uk/cosmic/>). Another database oncoKB[23]  
229 (<https://oncokb.org/>), which has a list of 1,064 cancer genes, was added as a supplement to  
230 COSMIC CGC genes. Oncogenic signaling pathways were provided by the cBioPortal  
231 database[24] (<http://www.cbioportal.org/>). Statistical analysis and visualization were  
232 performed in R (v3.6.3) using packages ggplot2 (v3.3.2), networkD3 (v0.4). For novel  
233 candidates, we used three types of biological interpretation (Gene Oncology, Pathways, and  
234 Protein-Protein Interaction) to obtain biological knowledge.

235

## 236 **Statistical methods**

237 We employed an approach as described previously [10, 18] to evaluate the correlation between  
238 eRNAs and irAE RORs or ORRs. Linear-regression models for predicting irAE ROR or ORR  
239 across cancer types, was constructed by the R function lm, and the performance of the  
240 prediction was estimated based on Spearman rank correlation, using the R package psych  
241 (v2.0.12). To compare the goodness of fit between different models, a log-likelihood ratio test  
242 was performed using the R package lmttest (v0.9). We compute variance inflation factor (VIF)  
243 to assess multicollinearity using the vif function from the R package car (v3.0) to exclude  
244 combinations containing highly correlated factors.

245

## 246 Acknowledgements

247 The research has been supported by National Natural Science Foundation of China (NSFC)  
248 (Grant 31571350, U1611265, and 31871323). The results shown here are in whole or part  
249 based upon data generated by the TCGA or CPTAC Research Network.

250

## 251 Conflict of Interests

252 The authors declare no competing interests.

253

## 254 Author contributions

255 YYX and MBG conceived and supervised the study. ZYL, YYX, and MBG performed the  
256 analysis. MBG drafted the manuscript with assistance from ZYL. YYX reviewed the  
257 manuscript. All authors approved the final manuscript.

258

## 259 References

260

261 1 Boussiotis VA. Molecular and Biochemical Aspects of the PD-1 Checkpoint  
262 Pathway. *N Engl J Med* 2016; 375: 1767-1778.

263

264 2 Dong H, Strome SE, Salomao DR, Tamura H, Hirano F, Flies DB *et al.* Tumor-  
265 associated B7-H1 promotes T-cell apoptosis: a potential mechanism of immune  
266 evasion. *Nat Med* 2002; 8: 793-800.

267

- 268 3 Sharpe AH, Pauken KE. The diverse functions of the PD1 inhibitory pathway. *Nat*  
269 *Rev Immunol* 2018; 18: 153-167.  
270
- 271 4 Keir ME, Butte MJ, Freeman GJ, Sharpe AH. PD-1 and its ligands in tolerance and  
272 immunity. *Annu Rev Immunol* 2008; 26: 677-704.  
273
- 274 5 Topalian SL, Hodi FS, Brahmer JR, Gettinger SN, Smith DC, McDermott DF *et al.*  
275 Safety, activity, and immune correlates of anti-PD-1 antibody in cancer. *N Engl J*  
276 *Med* 2012; 366: 2443-2454.  
277
- 278 6 Patel SP, Kurzrock R. PD-L1 Expression as a Predictive Biomarker in Cancer  
279 Immunotherapy. *Mol Cancer Ther* 2015; 14: 847-856.  
280
- 281 7 Yarchoan M, Hopkins A, Jaffee EM. Tumor Mutational Burden and Response Rate to  
282 PD-1 Inhibition. *N Engl J Med* 2017; 377: 2500-2501.  
283
- 284 8 Le DT, Durham JN, Smith KN, Wang H, Bartlett BR, Aulakh LK *et al.* Mismatch  
285 repair deficiency predicts response of solid tumors to PD-1 blockade. *Science* 2017;  
286 357: 409-413.  
287
- 288 9 Yu X, Zhang Z, Wang Z, Wu P, Qiu F, Huang J. Prognostic and predictive value of  
289 tumor-infiltrating lymphocytes in breast cancer: a systematic review and meta-  
290 analysis. *Clin Transl Oncol* 2016; 18: 497-506.  
291

- 292 10 Lee JS, Ruppin E. Multiomics Prediction of Response Rates to Therapies to Inhibit  
293 Programmed Cell Death 1 and Programmed Cell Death 1 Ligand 1. *JAMA Oncol*  
294 2019.
- 295
- 296 11 Rooney MS, Shukla SA, Wu CJ, Getz G, Hacohen N. Molecular and genetic  
297 properties of tumors associated with local immune cytolytic activity. *Cell* 2015; 160:  
298 48-61.
- 299
- 300 12 Pitt JM, Vetizou M, Daillere R, Roberti MP, Yamazaki T, Routy B *et al.* Resistance  
301 Mechanisms to Immune-Checkpoint Blockade in Cancer: Tumor-Intrinsic and -  
302 Extrinsic Factors. *Immunity* 2016; 44: 1255-1269.
- 303
- 304 13 Chow LQM, Haddad R, Gupta S, Mahipal A, Mehra R, Tahara M *et al.* Antitumor  
305 Activity of Pembrolizumab in Biomarker-Unselected Patients With Recurrent and/or  
306 Metastatic Head and Neck Squamous Cell Carcinoma: Results From the Phase Ib  
307 KEYNOTE-012 Expansion Cohort. *J Clin Oncol* 2016; 34: 3838-3845.
- 308
- 309 14 Zandberg DP, Algazi AP, Jimeno A, Good JS, Fayette J, Bouganim N *et al.*  
310 Durvalumab for recurrent or metastatic head and neck squamous cell carcinoma:  
311 Results from a single-arm, phase II study in patients with  $\geq 25\%$  tumour cell PD-L1  
312 expression who have progressed on platinum-based chemotherapy. *Eur J Cancer*  
313 2019; 107: 142-152.
- 314

- 315 15 Weber JS, Hodi FS, Wolchok JD, Topalian SL, Schadendorf D, Larkin J *et al.* Safety  
316 Profile of Nivolumab Monotherapy: A Pooled Analysis of Patients With Advanced  
317 Melanoma. *J Clin Oncol* 2017; 35: 785-792.  
318
- 319 16 Wang DY, Salem JE, Cohen JV, Chandra S, Menzer C, Ye F *et al.* Fatal Toxic  
320 Effects Associated With Immune Checkpoint Inhibitors: A Systematic Review and  
321 Meta-analysis. *JAMA Oncol* 2018; 4: 1721-1728.  
322
- 323 17 Salem JE, Manouchehri A, Moey M, Lebrun-Vignes B, Bastarache L, Pariente A *et*  
324 *al.* Cardiovascular toxicities associated with immune checkpoint inhibitors: an  
325 observational, retrospective, pharmacovigilance study. *Lancet Oncol* 2018; 19: 1579-  
326 1589.  
327
- 328 18 Jing Y, Liu J, Ye Y, Pan L, Deng H, Wang Y *et al.* Multi-omics prediction of  
329 immune-related adverse events during checkpoint immunotherapy. *Nat Commun*  
330 2020; 11: 4946.  
331
- 332 19 Andersson R, Gebhard C, Miguel-Escalada I, Hoof I, Bornholdt J, Boyd M *et al.* An  
333 atlas of active enhancers across human cell types and tissues. *Nature* 2014; 507: 455-  
334 461.  
335
- 336 20 Leveille N, Melo CA, Agami R. Enhancer-associated RNAs as therapeutic targets.  
337 *Expert Opin Biol Ther* 2015; 15: 723-734.  
338

- 339 21 Zhang Z, Lee JH, Ruan H, Ye Y, Krakowiak J, Hu Q *et al.* Transcriptional landscape  
340 and clinical utility of enhancer RNAs for eRNA-targeted therapy in cancer. *Nat*  
341 *Commun* 2019; 10: 4562.
- 342
- 343 22 Tate JG, Bamford S, Jubb HC, Sondka Z, Beare DM, Bindal N *et al.* COSMIC: the  
344 Catalogue Of Somatic Mutations In Cancer. *Nucleic Acids Res* 2019; 47: D941-D947.
- 345
- 346 23 Chakravarty D, Gao J, Phillips SM, Kundra R, Zhang H, Wang J *et al.* OncoKB: A  
347 Precision Oncology Knowledge Base. *JCO Precis Oncol* 2017; 2017.
- 348
- 349 24 Cerami E, Gao J, Dogrusoz U, Gross BE, Sumer SO, Aksoy BA *et al.* The cBio  
350 cancer genomics portal: an open platform for exploring multidimensional cancer  
351 genomics data. *Cancer Discov* 2012; 2: 401-404.
- 352
- 353 25 Gao J, Aksoy BA, Dogrusoz U, Dresdner G, Gross B, Sumer SO *et al.* Integrative  
354 analysis of complex cancer genomics and clinical profiles using the cBioPortal. *Sci*  
355 *Signal* 2013; 6: p11.
- 356
- 357 26 Lappas M. RAF1 is increased in labouring myometrium and modulates inflammation-  
358 induced pro-labour mediators. *Reproduction* 2016; 151: 411-420.
- 359
- 360 27 Kraja AT, Chasman DI, North KE, Reiner AP, Yanek LR, Kilpelainen TO *et al.*  
361 Pleiotropic genes for metabolic syndrome and inflammation. *Mol Genet Metab* 2014;  
362 112: 317-338.
- 363

- 364 28 Chen Y, Wang YJ, Zhao Y, Wang JC. Carbohydrate response element binding protein  
365 (ChREBP) modulates the inflammatory response of mesangial cells in response to  
366 glucose. *Biosci Rep* 2018; 38.
- 367
- 368 29 Fujiwara T, Kofuji T, Akagawa K. Dysfunction of the hypothalamic-pituitary-adrenal  
369 axis in STX1A knockout mice. *J Neuroendocrinol* 2011; 23: 1222-1230.
- 370
- 371 30 Bagge A, Dahmcke CM, Dalgaard LT. Syntaxin-1a is a direct target of miR-29a in  
372 insulin-producing beta-cells. *Horm Metab Res* 2013; 45: 463-466.
- 373
- 374 31 Liang T, Qin T, Xie L, Dolai S, Zhu D, Prentice KJ *et al.* New Roles of Syntaxin-1A  
375 in Insulin Granule Exocytosis and Replenishment. *J Biol Chem* 2017; 292: 2203-  
376 2216.
- 377
- 378 32 Phee H, Au-Yeung BB, Pryshchep O, O'Hagan KL, Fairbairn SG, Radu M *et al.* Pak2  
379 is required for actin cytoskeleton remodeling, TCR signaling, and normal thymocyte  
380 development and maturation. *Elife* 2014; 3: e02270.
- 381
- 382 33 Gmyrek GB, Graham DB, Sandoval GJ, Blaufuss GS, Akilesh HM, Fujikawa K *et al.*  
383 Polarity gene discs large homolog 1 regulates the generation of memory T cells. *Eur J*  
384 *Immunol* 2013; 43: 1185-1194.
- 385
- 386 34 Dong X, Li X, Liu C, Xu K, Shi Y, Liu W. Discs large homolog 1 regulates B-cell  
387 proliferation and antibody production. *Int Immunol* 2019; 31: 759-770.
- 388

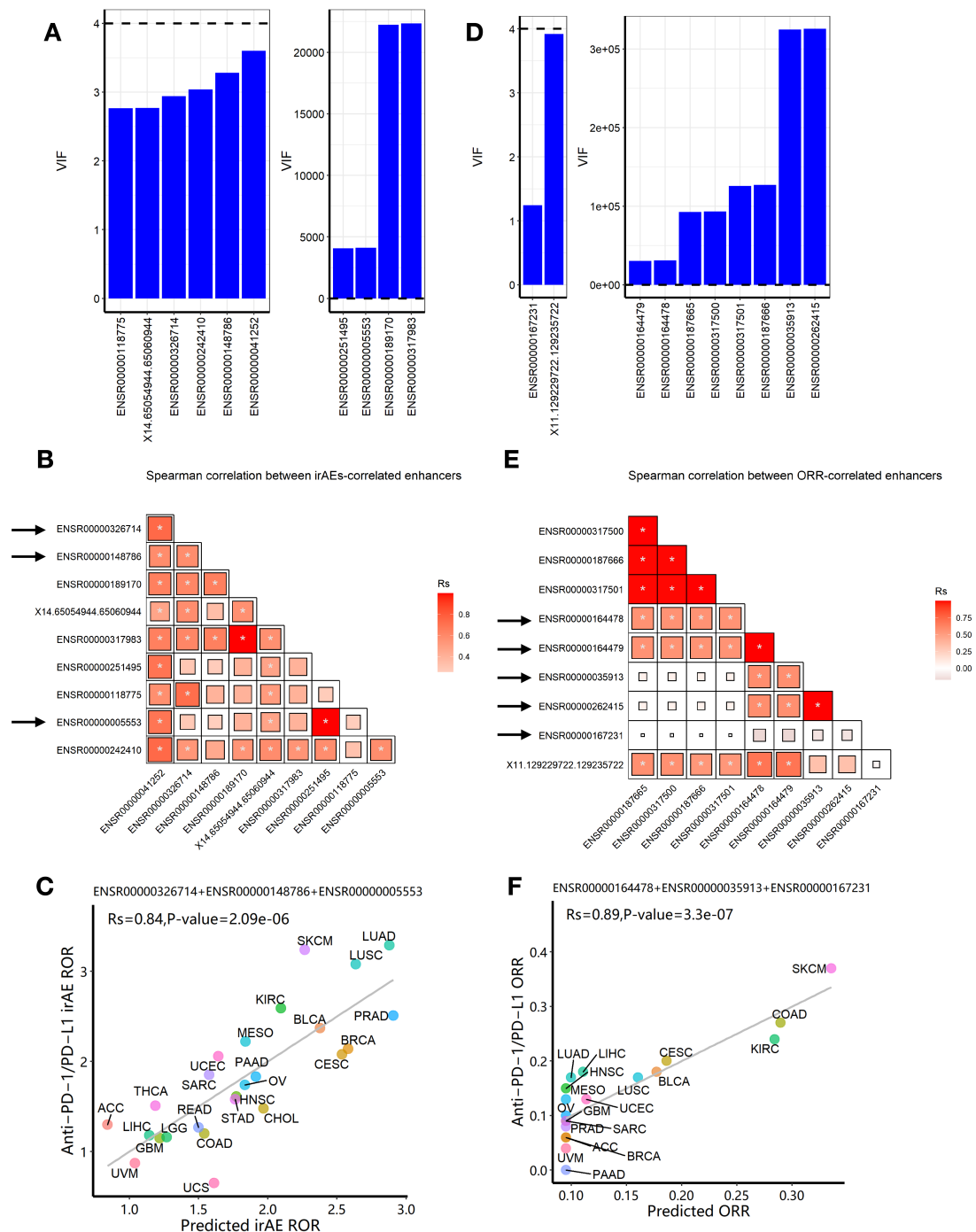


- 389 35 Hu B, Yang XB, Sang XT. Development and Verification of the Hypoxia-Related and  
390 Immune-Associated Prognosis Signature for Hepatocellular Carcinoma. *J Hepatocell*  
391 *Carcinoma* 2020; 7: 315-330.  
392
- 393 36 Bate A, Evans SJ. Quantitative signal detection using spontaneous ADR reporting.  
394 *Pharmacoepidemiol Drug Saf* 2009; 18: 427-436.  
395
- 396 37 Oshima Y, Tanimoto T, Yuji K, Tojo A. EGFR-TKI-Associated Interstitial  
397 Pneumonitis in Nivolumab-Treated Patients With Non-Small Cell Lung Cancer.  
398 *JAMA Oncol* 2018; 4: 1112-1115.  
399
- 400 38 Szklarczyk D, Gable AL, Lyon D, Junge A, Wyder S, Huerta-Cepas J *et al*. STRING  
401 v11: protein-protein association networks with increased coverage, supporting  
402 functional discovery in genome-wide experimental datasets. *Nucleic Acids Res* 2019;  
403 47: D607-D613.  
404
- 405 39 Yu G, Wang LG, Han Y, He QY. clusterProfiler: an R package for comparing  
406 biological themes among gene clusters. *OMICS* 2012; 16: 284-287.  
407
- 408 40 Huang da W, Sherman BT, Lempicki RA. Systematic and integrative analysis of large  
409 gene lists using DAVID bioinformatics resources. *Nat Protoc* 2009; 4: 44-57.  
410  
411  
412

413 Figure Legends

414

Fig. 1

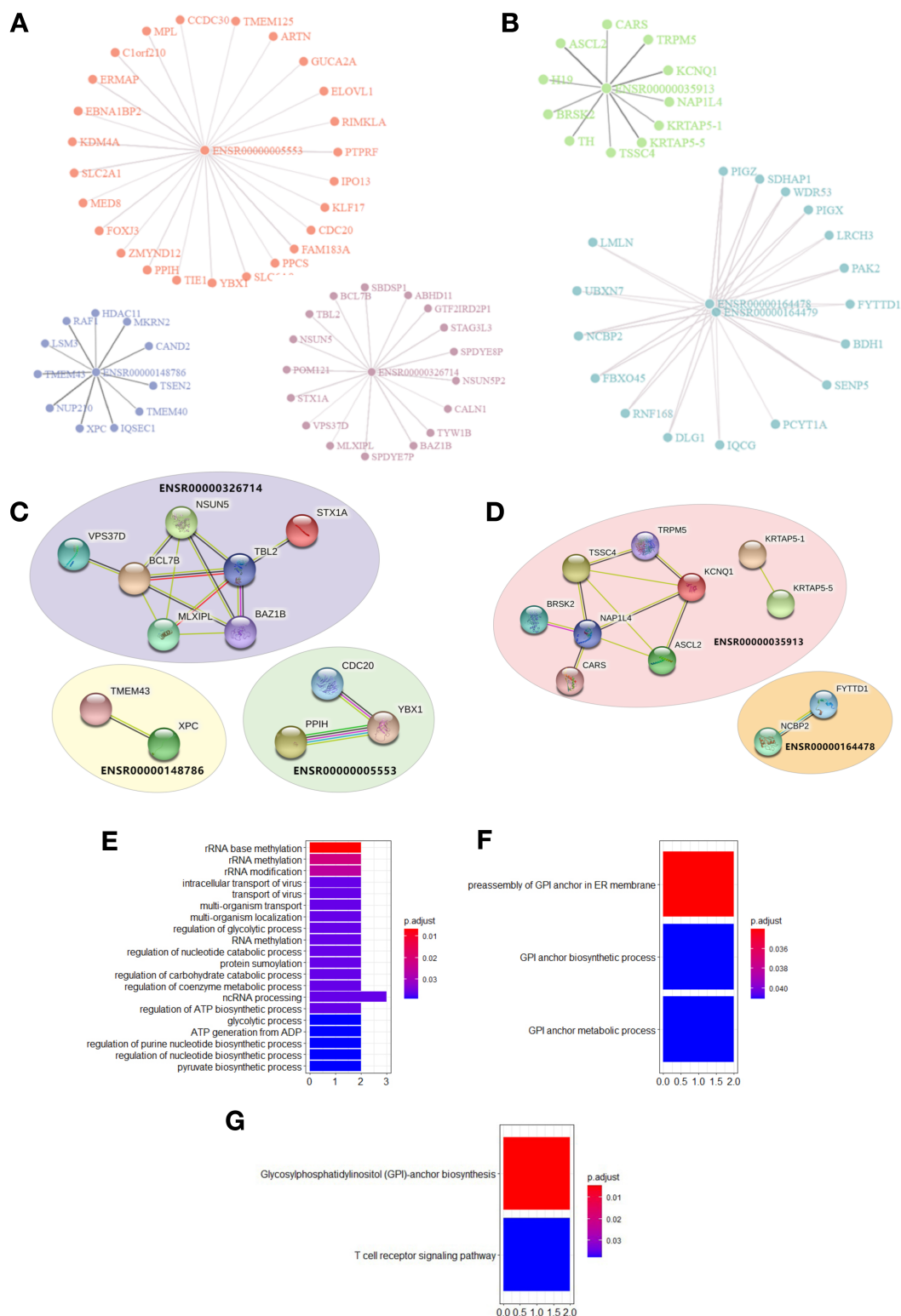


415 Fig.1, Construction of eRNA-based prediction models for irAE ROR (risk) and ORR  
 416 (benefit) of immunotherapy. (A) Multicollinearity (VIF) analysis for top ten eRNA  
 417 expression in predicting irAEs. Six eRNAs showed no multicollinearity, while 4 eRNAs

418 showed strong multicollinearity. **(B)** Spearman correlation between irAE-correlated eRNAs.  
419 Pairwise Spearman correlation ( $R_s$ ) of expression level between candidate eRNAs. The shade  
420 of the square indicates the  $R_s$ , and the size indicates P-value (\* indicates statistical significance  
421  $P < 0.05$ ). **(C)** Combined effect of ENSR00000326714, ENSR00000148786 and ENSR00-  
422 000005553 trivariate model of predicting irAEs ( $R=0.84$ ,  $P=2.1e-6$ ). The equation of the best  
423 trivariate model is  $0.1912*ENSR00000005553+0.4097*ENSR000-$   
424  $00326714+0.1953*ENSR00000148786+0.2942$ . **(D)** Multicollinearity analysis for top ten  
425 eRNA expression in predicting ORR. Two eRNAs showed no multicollinearity, while 8  
426 eRNAs showed strong multicollinearity. **(E)** Spearman correlation between ORR-correlated  
427 eRNAs. Spearman correlation ( $R_s$ ) of expression level was calculated between two candidate  
428 eRNAs. The shade of the square indicates the  $R_s$ , and the size indicates P-value (\* indicates  
429 statistical significance  $P < 0.05$ ). **(F)** Combined effect of ENSR00000164478,  
430 ENSR00000035913 and ENSR000-00167231 trivariate model of predicting ORR ( $R=0.89$ ,  
431  $P=3.3e-7$ ). The equation of the best trivariate model is  $0.0953+0.0649*$   
432  $ENSR00000164478+0.0032*$  ENSR00000035913+ $0.1687*$  ENSR00000167231. irAE,  
433 immune-related adverse events; ROR, reporting odds ratio; ORR, objective response rates;  
434 LUAD, lung adenocarcinoma; SKCM, skin cutaneous melanoma; LUSC, lung squamous cell  
435 carcinoma; KIRC, kidney renal clear cell carcinoma; PRAD, prostate adenocarcinoma; BLCA,  
436 bladder urothelial carcinoma; MESO, mesothelioma; BRCA, breast invasive carcinoma; CESC,  
437 cervical squamous cell carcinoma and endocervical adenocarcinoma; UCEC, uterine corpus  
438 endometrial carcinoma; SARC, sarcoma; ESCA, esophageal carcinoma; PAAD, pancreatic  
439 adenocarcinoma; OV, ovarian serous cystadenocarcinoma; HNSC, head and neck squamous  
440 cell carcinoma; STAD, stomach adenocarcinoma; THCA, thyroid carcinoma; CHOL,  
441 cholangiocarcinoma; ACC, adrenocortical carcinoma; READ, rectum adenocarcinoma; COAD,

442 colon adenocarcinoma; LIHC, liver hepatocellular carcinoma; LGG, brain lower-grade glioma;  
 443 GBM, glioblastoma multiforme; UVM, uveal melanoma; UCS, uterine carcinosarcoma.  
 444

Fig. 2



445

446 **Fig. 2.** Visualization of enhancer-target interaction network and functional enrichment. **(A)**

447 target genes of irAE-related enhancers ENSR0000005553, ENSR00000326714, and

448 ENSR00000148786. **(B)** target genes of ORR-related enhancers ENSR00000164478,

449 ENSR00000164479, and ENSR00000035913. **(C)** Protein-Protein Interaction (PPI) network

450 for target genes of irAE-related enhancer ENSR00000326714, ENSR00000148786,

451 ENSR0000005553; and their corresponding PPI of targets in irAE ROR model. **(D)** PPI

452 network for targets of ORR-related enhancers ENSR00000035913, ENSR000-00164478. **(E)**

453 GO enrichment of genes regulated by irAE-correlated enhancer ENSR00000326714. **(F)** GO

454 enrichment of genes regulated by ORR-correlated enhancer ENSR00000164478. **(G)** KEGG

455 pathway enrichment of genes regulated by ORR-correlated enhancer ENSR00000164478.

456